Metallicities & More at $z \geq 2$

Michael V. Lesniak III
AST 591
21 October 2005

"Evidence for Solar Metallicities in Massive Star-forming Galaxies at $z \geq 2$"

Shapley, Erb, Pettini, Steidel, & Adelberger ApJ 2004, 612, 108

Outline

- Metallicity relations
- The “redshift desert”
- Measuring metallicity
- Metallicity-Luminosity relation
- Masses & star formation rates of galaxies
- Paper adopts quantities:

H_0 = 70 km s^{-1} Mpc^{-1}, $\Omega_m = 0.3$, $\Omega_\Lambda = 0.7$

Metallicity Correlations

- Locally, HII regions display relation between oxygen abundances and optical luminosity
  - More luminous → more metals
- Galaxies at $0.6 < z < 0.8$ are 1-3 mag more luminous than local galaxies of same metallicity (Kobulnick et al. 2003)
  - Faintest galaxies are most evolved
- Galaxies at $0.47 < z < 0.92$ have similar metallicities as those in local universe (Lilly et al. 2003)

Metallicity Correlations

- HII regions in 6 galaxies at $z > 2.5$ have (O/H) ~ 0.1-1.0(O/H)$_\odot$ but are 2-4 times as luminous
- Limited data of galaxies between z = 1.4 & z = 2.5
  - "Redshift desert"
  - Critical epoch of heavy element formation?

Anatomy of a Sample

- Objects analyzed from Steidel's 2004 survey
  - Selected star-forming galaxies at z ~ 2 from U_n-G vs. G-$\mathcal{R}$ plot
- Q1623 field of survey contains 167 galaxies at z > 1.4
  - 121 detected in K_s-band
  - For z > 1.9, K_s-band contains Hα and [NII] emission lines and corresponds to rest frame $\mathcal{R}$-band

Special Filters:

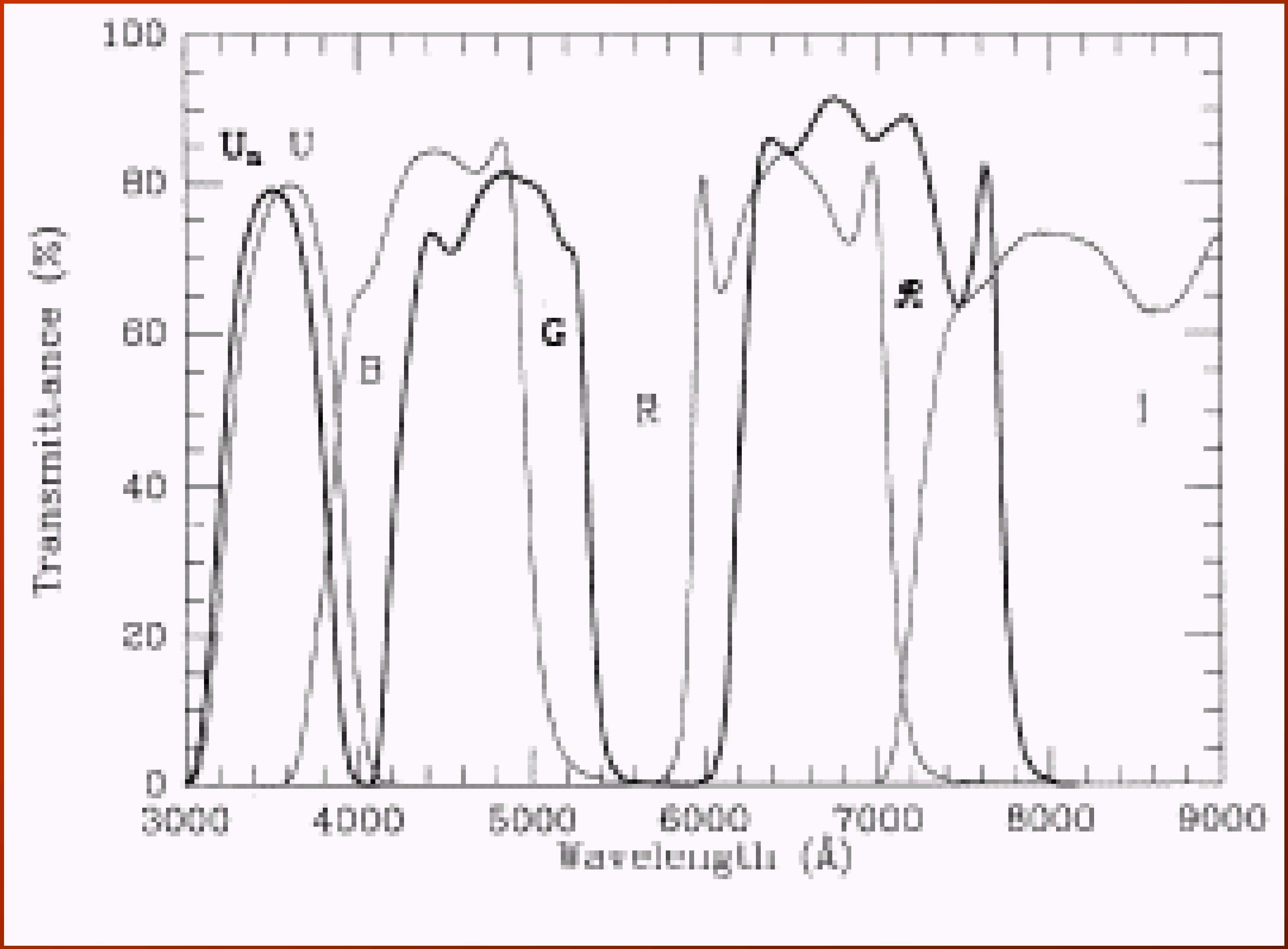

Steidel 1993 AJ, 105, 2017

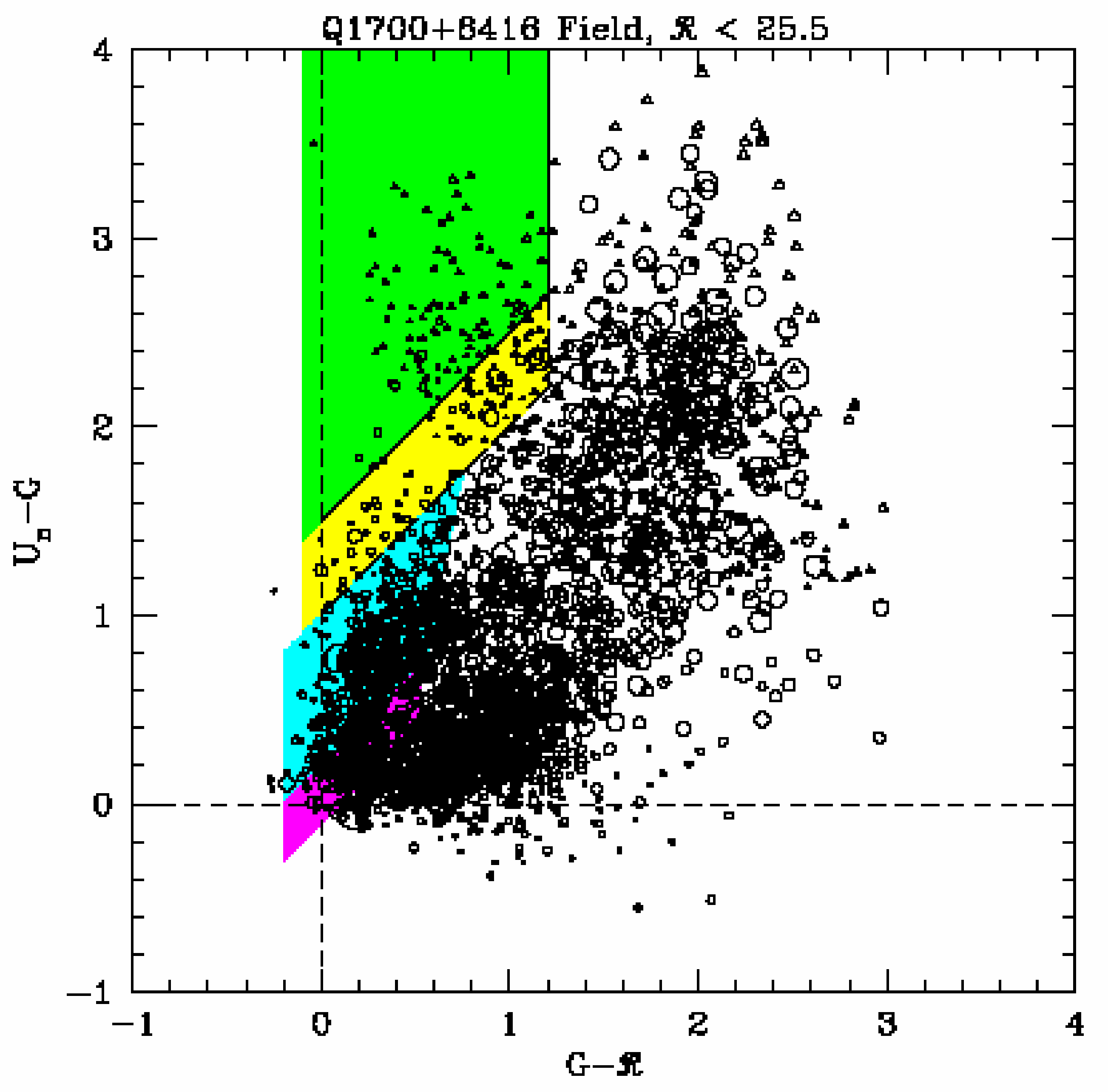

Steidel et al. ApJ 2004, 604, 534

Anatomy of a Sample

- Selected galaxies that in rest-frame would be optically bright ($K_s \leq 20$)
  - 9 galaxies fit criteria and were selected (8 successfully imaged)
  - 8 of 9 galaxies are “BX” objects
  - The last is an “MD” object

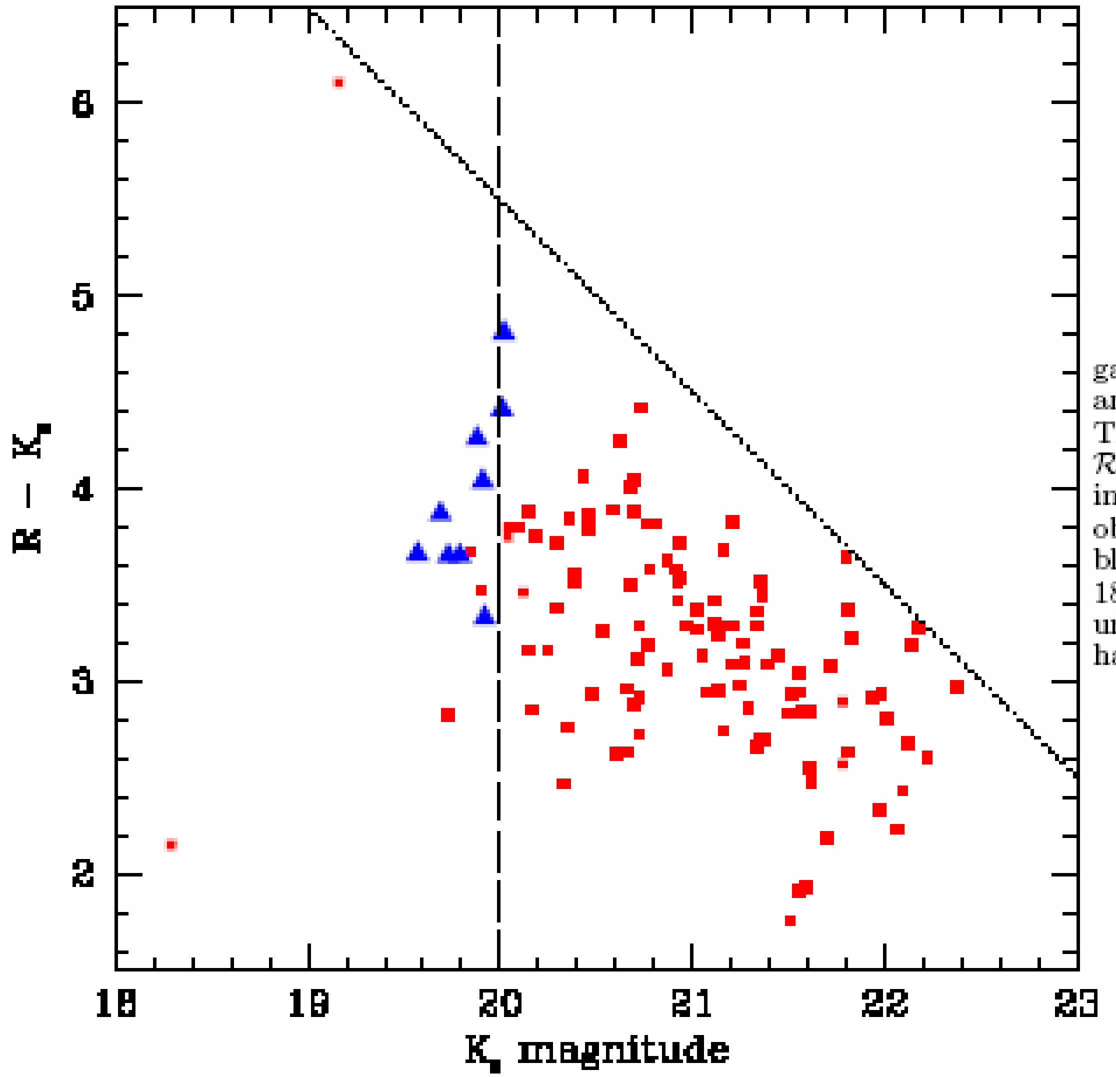

FIG. 1.— The Color-magnitude diagram of 121 UV-selected galaxies at $z > 1$ ($\langle z \rangle = 2.28 \pm 0.28$), in the Q1623 field. $\mathcal{R}$ and K_s magnitudes are on the AB and Vega systems, respectively. The dotted diagonal line indicates the survey magnitude limit of $\mathcal{R} = 25.5$. Only $\sim 10\%$ of the objects at $z > 1$ also have $K_s \leq 20.0$, indicated by the long-dashed line. The nine $K \leq 20.0$ objects observed with NIRSPEC in September 2003 are indicated by large blue triangles. The object in the lower left-hand corner, with $K_s = 18.29$ and $\mathcal{R} - K_s = 2.15$, is a QSO at $z = 2.529$. The median color uncertainty is $\sigma(\mathcal{R} - K_s) = 0.25$, though the 10 K_s-selected objects have $\sigma(\mathcal{R} - K_s) \sim 0.10$.

Determining Metallicity

- R_{23} method most common
  - Find ratio ([OII]+[OIII])/Hβ
  - Needs an independent ratio to determine whether a galaxy is metal-rich or metal-poor
- At z ~ 2, [NII] lines are in optical region
  - Use ratio of [NII]λ6584/Hα (Pettini & Pagel 2004)
  - Relate nitrogen abundances to oxygen

Table 1. Galaxies Observed With Keck II/NIRSPEC

Galaxy	R.A. (J2000)	Dec. (J2000)	$z_{Ly\alpha}$ [a]	z_{abs} [b]	$z_{H\alpha}$ [c]	$\mathcal{R}_{AB}$	$(G-\mathcal{R})_{AB}$	$(U_n-G)_{AB}$	$\mathcal{R}_{AB}-K_{s,Vega}$	Exposure (s)
Q1623-BX274	16 25 38.202	26 45 57.141	2.415	2.408	2.4100	23.23	0.25	0.89	3.66	3×900
Q1623-MD66	16 25 40.392	26 50 08.878	...	2.111	2.1075	23.95	0.37	1.40	4.04	3×900
Q1623-BX341	16 25 43.554	26 46 36.942	...	2.377	...	24.83	0.47	0.90	4.81	2×900
Q1623-BX344[d]	16 25 43.931	26 43 41.977	...	2.422	2.4224	24.42	0.39	1.25	4.41	2×900
Q1623-BX453	16 25 50.836	26 49 31.399	2.183	2.171	2.1816	23.38	0.48	0.99	3.65	3×900
Q1623-BX513	16 25 55.856	26 46 50.304	2.249	2.244	2.2473	23.25	0.26	0.68	3.33	2×900
Q1623-BX528	16 25 56.439	26 50 15.444	...	2.266	2.2682	23.56	0.25	0.71	3.87	4×900
Q1623-BX599	16 26 02.545	26 45 31.900	...	2.329	2.3304	23.44	0.22	0.80	3.65	4×900
Q1623-BX663[e]	16 26 04.576	26 48 00.202	2.435	...	2.4333	24.14	0.24	1.02	4.26	3×900

[a] Vacuum heliocentric redshift of Lyα emission line, when present.
[b] Vacuum heliocentric redshift from rest-frame UV interstellar absorption lines.
[c] Vacuum heliocentric redshift of Hα emission line.
[d] BX344 was observed with a $0\farcs57$ slit, while all other galaxies were observed with a $0\farcs76$ slit.
[e] The Hα emission in BX663 has a two distinct peaks, one at $z = 2.4333$, as listed above, and another at $z = 2.4289$.

Results

- Took spectra of 8 galaxies with NIRSPEC
- One galaxy tossed out due to OH contamination (BX 513)
- Detected Hα, [NII] emission, and [SII] emission
- 5 of 7 galaxies have $\sigma > 114$ km s^{-1}
  - 114 km s^{-1} is z ~ 2 avg. (Erp et al. 2004)

Results

- Mean Hα flux:
  $(1.34 \pm 0.50) \times 10^{-16}$ ergs cm^{-2}
- Star formation rate: $47 \pm 15\ M_{\odot}\ yr^{-1}$
- Values are 3 times greater than measured in Erp et al. (2003)
- Hα emission accounts for ~15% of K_s-band flux

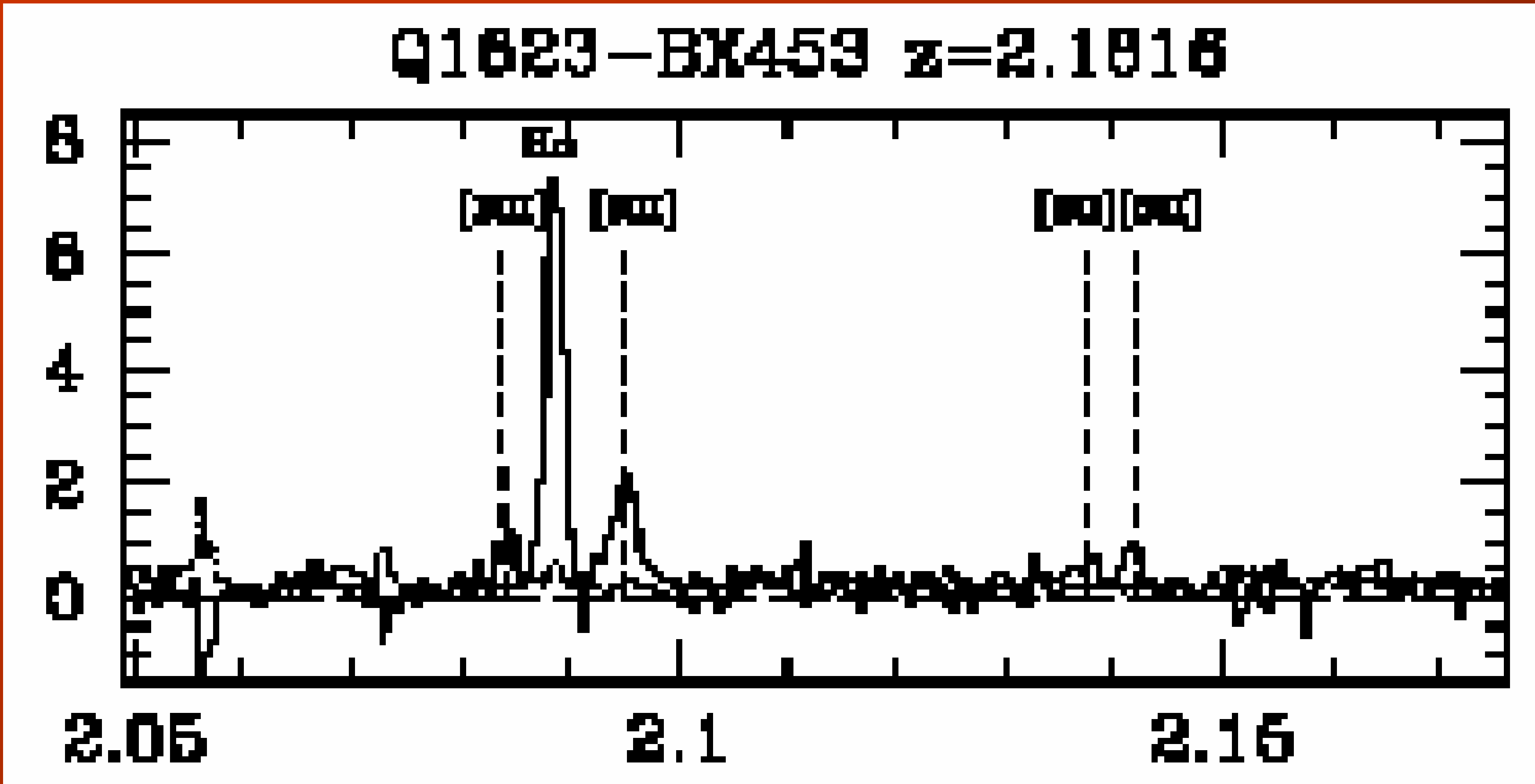

Q1623-BX453 z=2.1816
8
6
4
2
0
2.05
2.1
2.15

Results

- [N II]/Hα ratios measured from spectra
  - Mean value: 0.27
  - Data from Erp et al. 2003 yields mean of 0.10
- Given spectra S/N, all but one have ratios higher than minimum detectable (BX 528 measured [N II]/Hα = 0.19)
- Two galaxies had resolvable Hα profiles

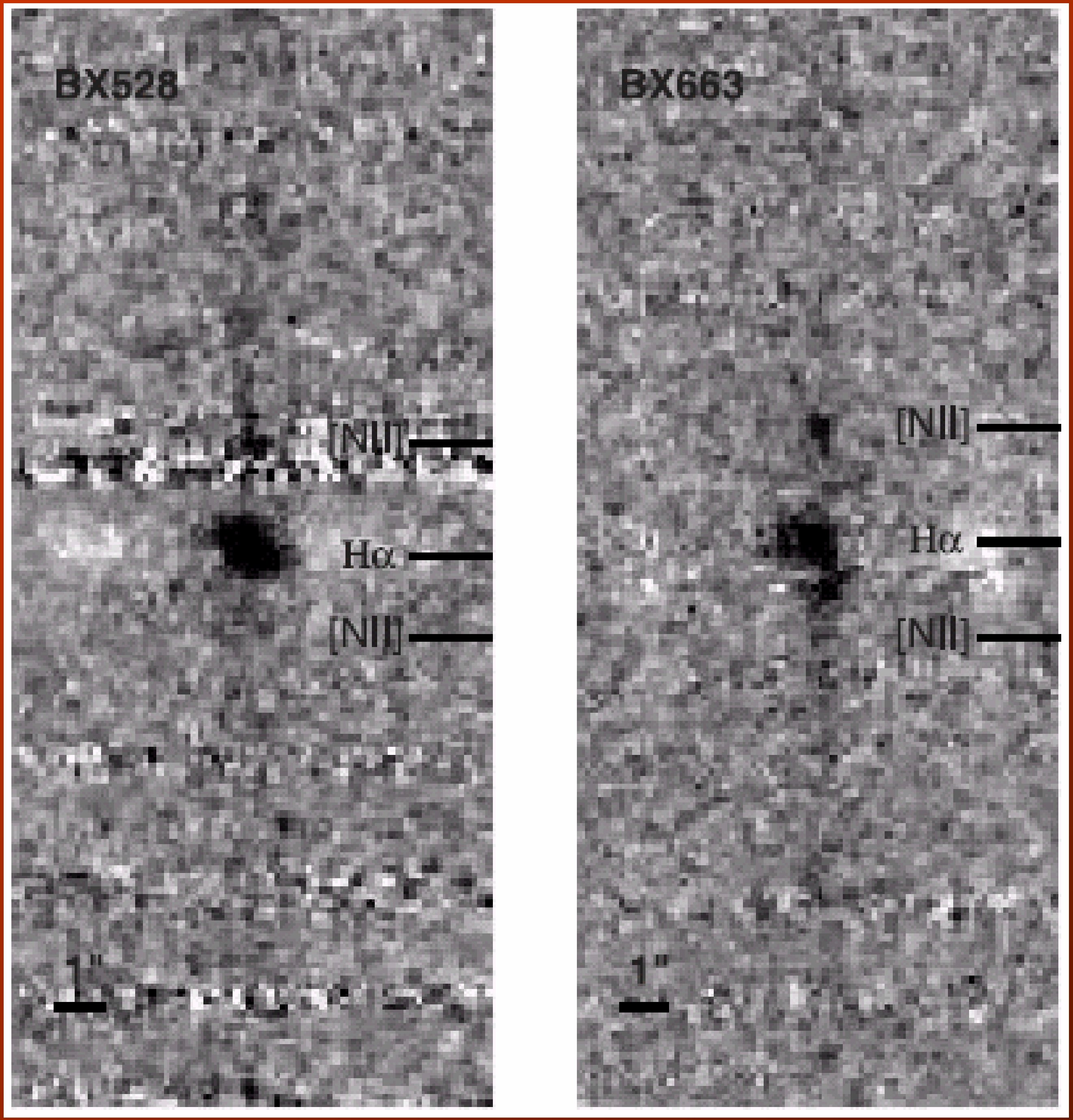
BX528
[NII]
Hα
[NII]
1"
BX663
[NII]
Hα
[NII]
1"

Oxygen Abundance

- Define: $N2 = \log([\text{N II}]\lambda 6584/\text{H}\alpha)$
- Two *N*2 to (O/H) relationships

  $12 + \log(\text{O/H}) = 8.90 + 0.57N2$

  - From Pettini & Pagel 2004
  - Results within 0.18 dex (68% confidence)

  $12 + \log(\text{O/H}) = 9.12 + 0.73N2$

  - From Denicolo et al. 2002
- For comparison:
  - Solar abundance: $12 + \log(\text{O/H}) = 8.66 \pm 0.05$
  - Orion Nebula: $12 + \log(\text{O/H}) = 8.64 \pm 0.06$

TABLE 2

Hα AND [N II] MEASUREMENTS AND THE ABUNDANCE OF OXYGEN

Galaxy	$z_{H\alpha}$ [a]	σ [b] (km s^{-1})	$F_{H\alpha}$ [c]	$F_{[N II]}$ [c]	[N II]/Hα	12 + log (O/H) [d]	12 + log (O/H) [e]
Q1623-BX 274	2.4100	121 ± 10	9.5 ± 0.4	1.6 ± 0.4	0.17 ± 0.04	8.47 ± 0.19	8.56 ± 0.21
Q1623-MD 66..................	2.1075	120 ± 5	19.7 ± 0.4	3.4 ± 0.4	0.17 ± 0.02	8.47 ± 0.18	8.57 ± 0.20
Q1623-BX 344	2.4224	92 ± 9	17.1 ± 0.7	6.2 ± 0.8	0.36 ± 0.05	8.65 ± 0.18	8.80 ± 0.20
Q1623-BX 453[f]	2.1816	61 ± 6	13.8 ± 0.3	4.1 ± 0.3	0.30 ± 0.02	8.60 ± 0.18	8.74 ± 0.20
Q1623-BX 513	2.2473	...[g]	3.3 ± 0.3	<0.9	<0.30	<8.60	<8.73
Q1623-BX 528	2.2682	142 ± 19	7.7 ± 0.5	1.5 ± 0.5	0.19 ± 0.07	8.49 ± 0.20	8.60 ± 0.23
Q1623-BX 599	2.3304	162 ± 9	18.1 ± 0.6	4.7 ± 0.6	0.26 ± 0.03	8.57 ± 0.18	8.69 ± 0.20
Q1623-BX 663	2.4333	132 ± 15	16.8 ± 0.9[h]	3.5 ± 0.3[h]	0.43 ± 0.05[h]	8.69 ± 0.18	8.85 ± 0.20

[a] Vacuum heliocentric redshift of Hα emission.

[b] Hα velocity dispersion obtained by fitting a Gaussian profile to the Hα line and deconvolving the effects of instrumental resolution.

[c] Line flux and random error in units of 10^{-17} ergs^{-1} cm^{-2}. While the systematic flux uncertainties are ~25%, the uncertainty in the [N II]/Hα flux-ratio is determined by the random errors in both line fluxes.

[d] Oxygen abundance deduced from the relationship presented in Pettini & Pagel (2004). For comparison, the most recent estimate of the solar abundance is $12 + \log(O/H)_{\odot} = 8.66 \pm 0.05$, and that of the Orion Nebula is $12 + \log(O/H)_{Orion} = 8.64 \pm 0.06$ (Allende Prieto et al. 2002; Asplund et al. 2004; Esteban et al. 1998).

[e] Oxygen abundance deduced from the relationship presented in Denicoló et al. (2002).

[f] The Hα and [N II] line fluxes presented are integrals under Gaussian fits to the lines, whose central wavelengths and FWHM are determined by the parameters of the Hα line. For all objects except BX 453, the fluxes obtained from the fits to the lines agree with the nonparametric integrals under the spectra, well within the uncertainties. However, in the case of BX 453, the [N II] flux obtained from the fit is 30% lower than that obtained by integrating nonparametrically under the spectrum, as a result of the larger apparent FWHM of the [N II] line than the Hα line.

[g] The Hα emission from BX 513 falls directly on top of a skyline, preventing a measurement of σ.

[h] The Hα line flux listed for BX 663 represents the sum of the two components integrated over the entire extended region of Hα emission. The [N II] line flux and [N II]/Hα ratio correspond to the more significantly detected, higher redshift component and only include flux from the spatial extent common to both transitions.

Oxygen Abundance

- Relationship adopted between [N II] and (O/H) is linear, but [N II] saturates at (O/H) $\geq$ (O/H)$_{\odot}$ and turns over beyond
  - Supersolar abundances?
- [N II]/Hα could be high, due to ignoring diffuse ionized gas contributions
- Excitation from AGN?
  - Lyα emission not there
  - Other emission lines not there (Si IV, Ci IV, & N V)

Metallicity-Luminosity Relation

- Nearby galaxies exhibit increasing luminosity with increasing metallicity
  - Seen over factor of 100 in (O/H) and 11 mag in M_B
- Galaxies at $z > 2$ can have M_B calculated from best-fit model SEDs
- Lyman-break galaxies (LBGs) at $z \sim 3$ are overluminous
- Similar result seen for $z \sim 2$ galaxies in sample

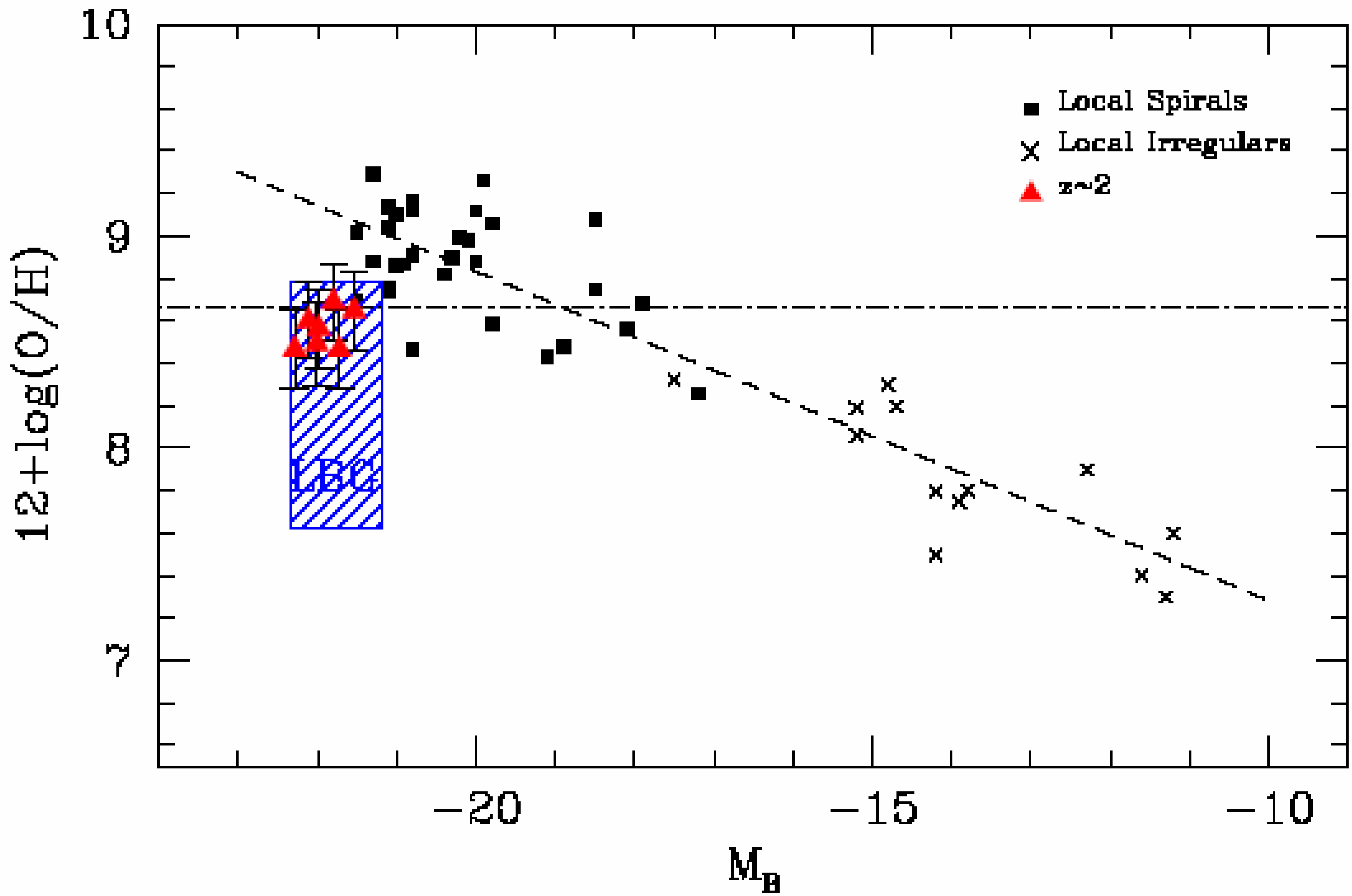

Fig. 4.— The Metallicity-Luminosity relationship. Data for local spiral (black squares) and irregular (black crosses) galaxies are taken from Garnett (2002), and display the well-studied strong correlation between (O/H) abundance and absolute B luminosity. The dashed line indicates a least-squares fit to the local data, while the dot-dashed line indicates solar (O/H) abundance. $K_s \leq 20.0$ UV-selected $z \sim 2$ objects (red triangles) are over-luminous for their (O/H) abundances, derived using the $N2$ calibration of Pettini & Pagel (2004), but lie closer to the relationship than $z \sim 3$ LBGs (blue shaded region). The majority of the $z \sim 2$ data points represent lower limits in (O/H), since the measured $N2$ values lie in a regime where this line ratio becomes insensitive to increasing metallicity.

Why Overluminous?

- Two different methods of calculating metallicity were used (R_{23} & $N2$)
  - Possible that *N*2-derived (O/H) too low and that real values are same as local universe
- Metallicities are likely to only grow toward present day
- Meier et al. (2004) proposes that (O/H) will increase and M_B will decrease toward present-day
  - However, future star formation rates cannot be accurately predicted

Why Overluminous?

- Need to expand sample-size to beyond $K_s \leq 20.0$
- Current sample has:
  - $<M_{\mathrm{opt}}> = -23.29$
  - $<[\mathrm{N\,II}]/\mathrm{H}\alpha> = 0.27$
  - $<12 + \log(\mathrm{O/H})> = 8.58$
- Erb et al. sample has:
  - $<M_{\mathrm{opt}}> = -22.16$
  - $<[\mathrm{N\,II}]/\mathrm{H}\alpha> = 0.10$
  - $<12 + \log(\mathrm{O/H})> = 8.33$

Stellar Masses & Ages

- Adopt Salpeter IMF
- Consider star-formation rates (SFRs) of form:
  - SFR(t) α exp($-t/\tau$)
- 5 of 7 galaxies appear to have formed $\geq 10^{11}$ $M_{\odot}$ of stars
- $\tau \geq$ 200 Myr required for models to fit
  - Significant fraction of Hubble time at $z \sim 2$
- Only models “casually” allowed by age of universe considered

TABLE 3. STAR-FORMATION RATES AND STELLAR POPULATION PARAMETERS

Galaxy	$z_{H\alpha}$ [a]	$L_{H\alpha}$ [b]	Uncorrected $SFR_{H\alpha}$ [c] ($M_\odot yr^{-1}$)	Uncorrected SFR_{UV} [d] ($M_\odot yr^{-1}$)	Model SFR[e] ($M_\odot yr^{-1}$)	$E(B-V)$ [f]	Age[g] (Gyr)	M_{star} [h] ($10^{11} M_\odot$)
Q1623-BX274	2.4100	4.3	34	28	75	0.12	1.3	1.9
Q1623-MD66	2.1075	6.5	51	10	65	0.23	0.9	0.9
Q1623-BX344	2.4224	7.9	62	8	49	0.20	1.6	1.9
Q1623-BX453	2.1816	4.9	39	16	174	0.27	0.4	0.9
Q1623-BX528	2.2682	3.0	24	18	44	0.11	1.7	1.9
Q1623-BX599	2.3304	7.6	60	22	49	0.10	1.3	1.3
Q1623-BX663	2.4333	7.8	62	12	33	0.13	2.0	2.3

[a] Vacuum heliocentric redshift of Hα emission.
[b] Hα luminosity in units of 10^{42} erg s^{-1}.
[c] SFR calculated from $L_{H\alpha}$, using the conversion of Kennicutt (1998).
[d] SFR calculated from L_{1500}, probed by the G apparent magnitude and using the conversion of Kennicutt (1998).
[e] SFR calculated by fitting a Bruzual & Charlot (2003) $\tau = 1$ Gyr model reddened by dust extinction to the $U_n G \mathcal{R} K_s$ colors of the galaxies. The best-fit value of $E(B-V)$ allows for the calculation of the dust-corrected value of the star-formation rate, listed here.
[f] The best-fit value of $E(B-V)$, assuming a Calzetti et al. (2000) dust-attenuation law as a function of wavelength.
[g] The best-fit value of stellar population age associated with the current episode of star formation, assuming an exponentially declining star-formation history with $\tau = 1$ Gyr.
[h] Formed stellar mass computed by integrating the best-fit exponentially-declining SFR between $t = 0$ and the best-fit age.

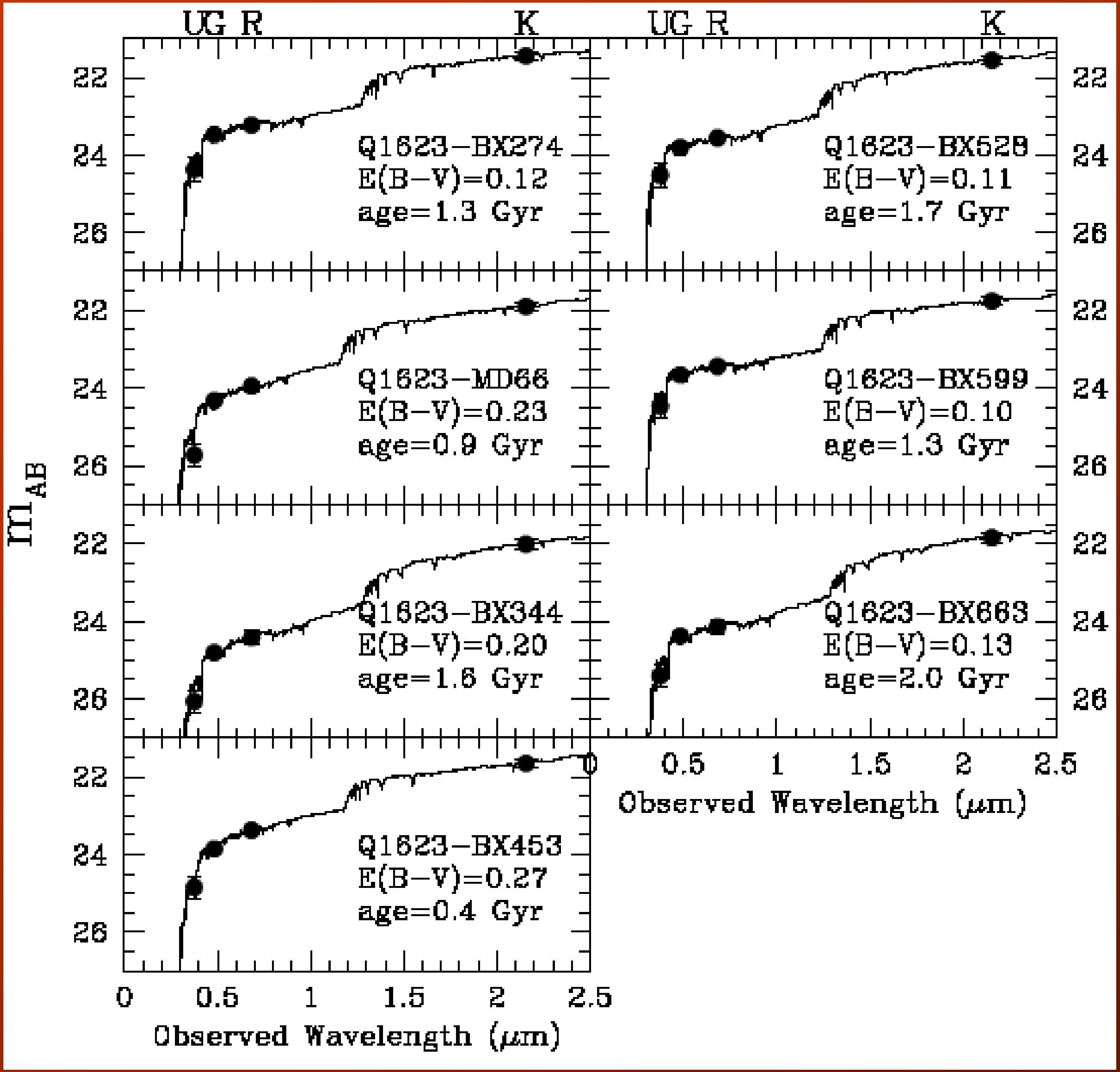
UG R
K
Q1623−BX274
E(B−V)=0.12
age=1.3 Gyr
Q1623−BX528
E(B−V)=0.11
age=1.7 Gyr
Q1623−MD66
E(B−V)=0.23
age=0.9 Gyr
Q1623−BX599
E(B−V)=0.10
age=1.3 Gyr
Q1623−BX344
E(B−V)=0.20
age=1.6 Gyr
Q1623−BX663
E(B−V)=0.13
age=2.0 Gyr
Q1623−BX453
E(B−V)=0.27
age=0.4 Gyr
m_{AB}
22
24
26
0
0.5
1
1.5
2
2.5
Observed Wavelength (μm)

Evolution between $z \sim 3$ & $z \sim 2$?

- Take a sample of z ~ 3 galaxies (Shapley et al. 2001) and evolve them to z ~ 2
  - $\tau = 1$ Gyr
  - $E(B-V)$ doesn't change
- Recalculate $\mathcal{R}$, K_s magnitudes and U_n-G, $G-\mathcal{R}$ colors
- Find that 15% of the $z \sim 3$ galaxies are possible progenitors of $z \sim 2$ galaxies in this sample

Stellar Mass Estimates

- Start with [NII]/Hα derived total masses
  - $\langle M_{star} \rangle = (1.4 \pm 0.5) \times 10^{11}\ M_{\odot}$
- Since the sample galaxies are among all other $z \sim 2$ galaxies on color plots, this mass is probably good for all $K_s \leq 20.0$, $z \sim 2$ systems
- Now estimate the number of bright galaxies without assigned redshifts that will lie in the redshift desert based on $\mathcal{R}$ magnitude

Stellar Mass Estimates

- Start with 2004 sample of 956 BX objects with known z and $\mathcal{R}$
- Bin BX galaxies by $\mathcal{R}$ magnitude and obtain fraction of galaxies in each bin that are in range of z (between 2.0 and 2.7)
- Bin systems with unknown z and $K_s \leq 20$ in Q1623 survey by $\mathcal{R}$ magnitude
- Multiply each Q1623 bin by its corresponding BX fraction

TABLE 4

FRACTION OF $2.0 \leq z \leq 2.7$ BX OBJECTS VERSUS $\mathcal{R}$ MAGNITUDE

$\mathcal{R}$ Magnitude Range (1)	Fraction of BX Objects with $2.0 \leq z \leq 2.7$[a] (2)	Q1623 BX Objects with $K_s \leq 20.0$ and No z (3)
$\mathcal{R} \leq 21.7$[b]	0/48	39
$21.7 < \mathcal{R} \leq 23.0$	6/51	13
$23.0 < \mathcal{R} \leq 24.0$	145/301	7
$24.0 < \mathcal{R} \leq 25.5$	386/556	8

[a] These statistics are based on the entire sample of 956 spectroscopically identified BX objects.

[b] We use $\mathcal{R} = 21.7$ as a cutoff since all spectroscopically confirmed BX objects at brighter magnitudes are stars and QSOs.

Result: 11 additional galaxies with $2.0 \leq z \leq 2.7$ and $K_s \leq 20$

Density at $z \sim 2$

- Number density of $2.0 \leq z \leq 2.7$ UV-selected objects with $K_s \leq 20.0$ in Q1623 is

  $n = 1.7 \times 10^{-4}\ \mathrm{Mpc}^{-3}$

- The mass density then is

  $\rho = n\langle M_{star}\rangle = (2.5 \pm 0.9) \times 10^{7}\ M_{\odot}\ \mathrm{Mpc}^{-3}$

- These galaxies represent ~10% of all BX objects at $z \sim 2$ so this is lower limit on density

K20 project

- Spectroscopic survey of ~500 $K_s \leq 20.0$ systems; 9 confirmed to be at $1.7 \leq z \leq 2.25$
- SFR ~ 100-500 $M_\odot$ yr^{-1}
- Star formation ages of 0.25-1.7 Gyr
- Stellar masses of (0.3-5.5) x 10^{11} $M_\odot$
- 4 are similar to this sample and have
  - E(B-V) = 0.3
  - Star formation ages of 0.7-1.7 Gyr

K20 project

- Space density of $1.7 \leq z \leq 2.25$ K20 systems: $n \approx 1.6 \times 10^{-4}$ Mpc^{-3}
- Stellar mass distributions are similar to Q1623 field

GDDS Survey

- Sample contains galaxies at $1.6 \leq z \leq 2.0$
- Adopting IMF that turns over below 0.5 $M_\odot$ (Baldry & Glazebrook 2003)
  - Masses of $6.3 \times 10^{10}\ M_\odot$
  - Mass density: $\rho = (1.7 \pm 0.6) \times 10^7\ M_\odot\ \mathrm{Mpc}^{-3}$
- To compare to this paper (Salpeter IMF), factor of 1.82 needed
  - After correction above values mirror results found in this paper

GDDS Survey - SSA22a field

- Field was observed in $U_n G \mathcal{R}$ filter set
- 3 confirmed galaxies at $1.6 \leq z \leq 2.0$, four maybe at $2.0 \leq z \leq 2.2$
- Most of these objects meet criteria for selection in this paper

Dynamical Masses

- Use Hα to obtain velocity dispersion
- Half-light radius determined from HST images: $r_{1/2}$ = 0.2-0.3 arcsec
- Assume spherical geometry
- Dynamical masses found via
  - $M_{dyn} = 5\sigma^2 r_{1/2}/G$
- These masses then compared to stellar masses calculated earlier

TABLE 5. COMPARISON OF DYNAMICAL AND STELLAR MASSES

Galaxy	σ[a] (km s^{-1})	M_{dyn}[b] ($10^{11} M_\odot$)	τ_{min}[c] (Gyr)	$M_{star}(\tau_{min})$[d] ($10^{11} M_\odot$)	τ_{max}[e] (Gyr)	$M_{star}(\tau_{max})$[f] ($10^{11} M_\odot$)
Q1623-BX274	121	0.28	0.20	1.27 (0.70)	5.00	2.76 (1.52)
Q1623-MD66	120	0.28	0.05	0.49 (0.27)	∞	1.19 (0.65)
Q1623-BX344	92	0.16	0.20	1.06 (0.58)	2.00	2.18 (1.20)
Q1623-BX453	61	0.07	0.01	0.49 (0.27)	∞	0.92 (0.51)
Q1623-BX528	142	0.58	0.20	1.09 (0.60)	2.00	2.47 (1.36)
Q1623-BX599	162	0.50	0.20	0.83 (0.46)	5.00	1.69 (0.93)
Q1623-BX663	132	0.45	0.20	1.06 (0.58)	1.00	2.35 (1.29)

[a] Hα velocity dispersion.
[b] Mass calculated from the Hα velocity dispersion.
[c] Minimum time-constant of models of the form $SFR(t) \propto \exp(-t/\tau)$ that provide statistically acceptable fits to the galaxy colors.
[d] Mass of best-fit model, assuming $\tau = \tau_{min}$. Values not in parentheses assume a Salpeter IMF extending down to $0.1 M_\odot$. Values in parentheses assume the more realistic Baldry & Glazebrook (2003) IMF, which has a break at $1 M_\odot$.
[e] Maximum time-constant of models for which the best-fit age is younger than the age of the universe. BX453 and MD66 can be fit by $\tau = \infty$, i.e. constant star-formation models, while the remaining galaxies' best-fit ages exceed that of the universe when $\tau = \infty$.
[f] Mass of best-fit model, assuming $\tau = \tau_{max}$. Values with and without parentheses have the same meaning as defined in note (d).

Mass Discrepancies

- If Salpeter IMF assumed, stellar mass exceeds dynamical mass in all cases
  - Extend radius beyond $r_{1/2}$ for M_{dyn}?
- Spherical symmetry probably not correct, one axis unequal to others requires correction
- Disklike shape introduces inclination effects
- Glazebrook IMF could be more appropriate

Loose ends

- Decrease uncertainty in metallicity using *O3N2* indicator, a ratio of ratios
  - *H*-band spectra needed for this
- To help discriminate the star formation models, ground-based *J*- and *H*-band and Spitzer observations could be used
- Higher confidence mass density values need wider range in luminosity

Summary

- 7 UV-selected z ~2 galaxies with $K_s \leq 20.0$ observed and analyzed
- High [NII]/Hα ratios found that yield solar and/or supersolar metallicities
- Galaxies are all overluminous for their metallicity, similar to z ~ 3 LBGs
- Galaxies have been forming stars over long timescales, contain $\geq 10^{11}$ $M_\odot$ and still have active star formation

Summary

- Results are roughly similar to two other surveys with overlapping redshifts
- Dynamically determined masses systematically lower than SED derived stellar masses